PAPER

Check for updates

Fully transient electrochemical testing strips for eco-friendly point of care testing†

Tingting Tu,[a] Bo Liang,*[a] Qingpeng Cao, [ID][a] Lu Fang,[b] Qin Zhu,[a] Yu Cai[a] and Xuesong Ye [ID] *[a]

With the growing number of patients suffering from noninfectious chronic diseases, the consumption of point of care testing strips increases exponentially, particularly blood glucose testing strips, causing an increasingly severe conflict between strip recycling and the environment. In this paper, fully transient electrochemical strips are developed as a substitute for non-degradable strips. Proper explorations were made, including finding out suitable degradable substrates for strip-making among different degradable materials and optimization of degradable conducting paste. Taking advantage of dissolvable polymer-based materials and nontoxic carbon materials, the transient strips have validated electrochemical functionality to determine physiological levels of glucose with a sensitivity of 14.33 μA mM^{-1} cm^{-2} (correlation coefficient R^2 is 0.99498) and reached full-degradation within a week after disposal. The interference experiment (negligible interference current response under 7%) and recovery tests (recovery ratio ranging from 92.46% to 102.47%) have illustrated its practical application in real sample detection. Such degradable-characterized testing strips can be widely used in chronic disease management with daily eco-friendly point of care testing, without potential pollution to the environment.

Introduction

With the development of the economy and the aggravation of aging, the prevalence of noninfectious chronic diseases (NCDs) is increasing. Patients with NCDs need to have clinical health management, especially self-management of medical treatment.[1,2] Point of care testing (POCT) using disposable strips is the most common way to monitor biochemical parameters (*e.g.*, glucose, uric acid, cholesterol, *etc.*) in human blood for NCD patients.[3] In the case of diabetes alone, according to the International Diabetes Federation (IDF), 425 million people suffer from diabetes globally.[4] For rough estimation, billions of disposable glucose testing strips are consumed and discarded every year. However, these commercialized testing strips are mostly made of polyethylene terephthalate (PET) and commercial conductive pastes, which are non-degradable and eco-harmful, causing a large amount of biomedical and plastic waste. Such waste must be appropriately managed and disposed of to protect the environment. Yet, treatment of these disposal strips can be troublesome because their use is widely distributed throughout the patients' daily life at home. Reducing or eliminating waste caused by the explosive growth of POCT strip consumption is a critical global environmental issue. Making these strips degradable may pave a new way to settle the environmental problem from the very beginning.

The idea of degradability has been widely applied in the medical domain. (*e.g.*, absorbable sutures). It was not introduced to the field of electronics until the first transient silicon electronic was proposed.[5] Studies focusing on degradable materials were widely investigated. Degradable materials are defined as a type of material that can maintain its full characteristics in regular use and be either physically or chemically destroyed when a trigger is applied. Conductors (*e.g.*, Zn, Mg, Fe, Mo, W),[6] semiconductors (Si, Ge, ZnO)[7,8] and dielectrics (MgO, SiO$_2$, Si$_3$N$_4$)[5,9] can all be dissolved in specific solutions despite their solubility differences. Their dissolution mechanism involves hydrolysis to form corresponding hydroxides because of their tendency to give away electrons.[5] Polymers (*e.g.*, silk fibroin,[10] poly(lactic-*co*-glycolic acid) (PLGA),[11] poly(vinyl alcohol) (PVA),[12] poly(caprolactone) (PCL),[13] polyvinylpyrrolidone (PVP),[14] *etc.*), water-soluble sodium carboxymethyl cellulose (Na-CMC)[15] and natural materials[16-18] (*e.g.*, egg albumen, natural pectin, natural wax) have been reported to serve as substrates or encapsulation layers of transient electronics. Even some dielectric materials such as SiO$_2$ and Si$_3$N$_4$ can be used for encapsulation.[9,19] As representative transient electronics, the devices reported by the Rogers group opened a gate to a new field.[5,11] Many transient devices have been developed including pressure sensor arrays,[20] temperature sensors,[11,21] pH sensors,[22] primary batteries,[23] supercapacitors,[24]

[a]*Biosensor National Special Laboratory, College of Biomedical Engineering and Instrument Science, Zhejiang University, Hangzhou 310027, PR China. E-mail: yexuesong@zju.edu.cn; boliang1986@zju.edu.cn*

[b]*College of Automation, Hangzhou Dianzi University, Hangzhou 310018, PR China*

radiofrequency (RF) circuit,[25] nanogenerators,[26] and electronics,[19,27] *etc.*, covering categories from sensors, implantable devices to energy harvesters.

While in the category of sensors, most devices are based on physical signal detection such as pressure sensors and temperature sensors. Recently, S. W. Hwang group developed a transient electrochemical dopamine monitor indicating a promising application of transient sensors in electrochemical detection field where rare researches were made.[13] The main challenge in this new field is that the electrodes of such a transient electrochemical sensor should be stable during detection in water or bio-fluid environment, in which materials above whether degradable conductors or polymers can be too active to remain unchanged. Take glucose detection for example, testing results can be available within one minute using commercial strips.[28] That is to say, the transient electrochemical testing strips should be stable for at least one minute while detecting other biochemical parameters may cost even longer time. In a word, the property of detection-steady is required for the transient electrochemical strip making. Meanwhile, in-time degradation is another essential goal that the strips should achieve.

In this paper, we developed an electrochemical testing strip with detection-steady and in-time degradation characteristics, which is perfectly suitable for eco-friendly POCT detection. The dissolution properties of four kinds of inexpensive and easy-available degradable substrates (Na-CMC, PVA, PVA/gelatin, PCL) were examined to find out an appropriate substrate material in this scenario. A degradable carbon paste composed of MWCNTs/carbon black (CB)/graphene and PLGA was put forward and optimized through proportional adjustment to obtain an ideal paste with satisfying conductivity and stability. Meanwhile, a set of electrochemical experiments of such a transient strip were performed including linear detection of glucose, anti-interference capability, and real sample detection. Ultimately, we successfully obtained a transient electrochemical strip with an ability to determine the physiological concentration of glucose indicating its potential application in eco-friendly blood glucose testing for daily diabetic management. The proposed transient electrochemical strips can also be developed for other biochemical parameters detection such as uric acid, cholesterol, *etc.*

Experimental

Reagents and materials

Sodium carboxymethyl cellulose (Na-CMC) (M_w: 250 000 g mol^{-1}) was purchased from Sigma-Aldrich (Shanghai, China). Poly(vinyl alcohol) (PVA) (PVA-1799), poly(caprolactone) (PCL, M_w: 80 000 g mol^{-1}), potassium ferricyanide (K$_3$[Fe(CN)$_6$]), ascorbic acid (AA), dopamine (DA), uric acid (UA), lactic acid (LA), multi-walled carbon nanotube (MWCNT) (>95%, OD: 8–15 nm, length: ~50 μm) and glucose oxidase (GOx, >180 U mg^{-1} protein, from *Aspergillus niger*) were purchased from Aladdin Biochemical Technology (Shanghai, China). Poly(lactic-*co*-glycolic acid) (PLGA) (M_w: 5000, PLA : PGA = 50 : 50) were purchased from Daigang Biomaterial (Jinan, China).

Chloroform, gelatin, HCl, BSA and glucose were purchased from Sinopharm Chemical Reagent (China). Graphene nanosheet (sheet diameter: 5–10 μm) and conductive carbon black (CB) (particle size: 30–45 nm) were all from Xianfeng Nanomaterials Technology (Nanjing, China). PBS solution (1 × 10^{-2} M, pH = 7.4) was purchased from Sangon Biotech (Shanghai, China). All aqueous solutions were prepared with deionized water (DI, 18 MΩ, ELGA-PURELAB).

Apparatus

All the morphology images were characterized by field emission scanning electron microscope (GEMINI 300). All the electrochemical measurements were performed using a μAutolab (TYPE 3) electrochemical workstation.

Preparation of degradable substrates

Dissolve Na-CMC (1.6 g) in DI water (20 mL) by magnetically stirring at 600 rpm until it was bubble-free (usually more than 3 hours) to make a homogeneous Na-CMC solution. To prepare PVA solution, add PVA (3 g) into DI water (20 mL) and stirred at 95 °C for 3 hours. Aqueous HCl solution (1 M, 10 mL) was added to expedite the dissolution. PVA/gelatin solution was prepared by stirring PVA (1 g) and gelatin (2 g) together in DI water (20 mL) at 95 °C for 3 hours. As for PCL solution, chloroform (20 mL) was used as a solvent for PCL (3 g). Solution casting method was employed using a Teflon mould (80 × 150 mm, 3 mm) for all the solutions above to fabricate four corresponding substrates. The casts were dried under ambient condition for 3 days before being carefully peeled-off from the mould.

Preparation of degradable carbon paste

Poly(lactic-*co*-glycolic acid) (PLGA), graphene nanosheets, multi-walled carbon nanotube (MWCNT) and conductive carbon black (CB) were used as received. Dissolve PLGA (0.6 g) in chloroform to form PLGA solution. Mechanically mix MWCNTs (0.06 g), graphene nanosheets (0.015 g) and CB (0.24 g) together in PLGA solution until degradable ink is suitable for stencil masking.

Glucose oxidase modification

To prepare the GOx solution, dissolve glucose oxidase (3 mg), K$_3$[Fe(CN)$_6$] (82.3125 mg) and BSA (1 mg) in PBS solution (1 × 10^{-2} M, pH = 7.4, 1 mL) to form a uniform enzyme solution with a concentration of 500 U mL^{-1}. Each strip was drop-casted with 2.5 μL enzyme solution on the sensing area using a micro syringe and stored at 4 °C overnight before detection.

Dissolution experiments of different substrates

Na-CMC, PVA, PVA/gelatin and PCL substrates were cut into small pieces of samples (10 × 20 mm) respectively. Centrifuge tubes served as sample containers (one sample each). Fill the centrifuge tube with DI water (4 mL) to immerse the sample for 10 min, 30 min, 2 h, 12 h, 1 d, 3 d, 10 d and 14 d. After that, dry them in a drying oven at 45 °C for 48 hours. Both the mass of containers and the samples were measured before and after
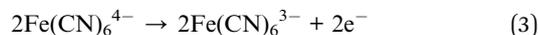
immersion. The dissolution rate was defined and determined as the ratio of the sample's mass loss to the initial mass (detailed definition in ESI†).

Results and discussion

A transient electrochemical strip with fully degradable components Fig. 1 unfolds an exploded view of a transient electrochemical testing strip based on fully degradable materials. The transient electrochemical testing strip consists of an encapsulation layer, a sensing system together with a flexible substrate with full-degradable characteristics.

As the most important part of the strip, the sensing system composed of degradable conducting traces and electrodes is printed onto the substrate through stencil mask printing. The sensing system is a typical three-electrode electrochemical system with working, reference and counter electrode (WE, RE and CE) made from degradable carbon paste (PLGA/MWCNTs/CB/Graphene). Ag/AgCl was not chosen for reference electrodes because of its high toxicity ranking to the environment as Ag^+ is one of the most toxic forms of heavy metals.[29] On the round-shaped area of the sensing system (WE), coated enzyme or antibodies, which served as an active sensing material. In the case of glucose detection, glucose oxidase solution is dropcasted onto this area to fulfil the corresponding enzymatic reaction. The magnified area of Fig. 1 (bottom left) expounds

a fundamental mechanism responsible for glucose detection applied in this paper. It can be described by the following equations:

$$Glucose + GOx(ox) \rightarrow gluconic\ acid + GOx(red) \quad (1)$$

$$GOx(red) + 2Fe(CN)_6^{3-} \rightarrow GOx(ox) + 2Fe(CN)_6^{4-} + 2 \quad (2)$$

$$2Fe(CN)_6^{4-} \rightarrow 2Fe(CN)_6^{3-} + 2e^- \quad (3)$$

The first reaction is the enzymatic reaction (eqn (1)) with glucose turning into gluconic acid under the help of GOx and reducing the GOx to the corresponding reduced form. The reduced form of GOx then reacts with the ferricyanide ($Fe(CN)_6^{3-}$), generating the oxidized form of GOx back and the reduced form of ferricyanide ($Fe(CN)_6^{4-}$). The ferricyanide here serves as an artificial mediator, the reduced form ($Fe(CN)_6^{4-}$) is then reoxidized on the surface of the electrode, giving a current signal proportional to the glucose concentration while regenerating the oxidized form of the mediator ($Fe(CN)_6^{3-}$).[30]

The whole fabrication process of this fully transient electrochemical strip is also presented in Fig. 1 (top). Both the encapsulation layer and the substrate were prepared by degradable material (PVA/gelatin) through solution casting method. Stencil mask printing was employed to produce the sensing system on the substrate. The encapsulation layer was later placed on the top of the sensing system as a cover of the
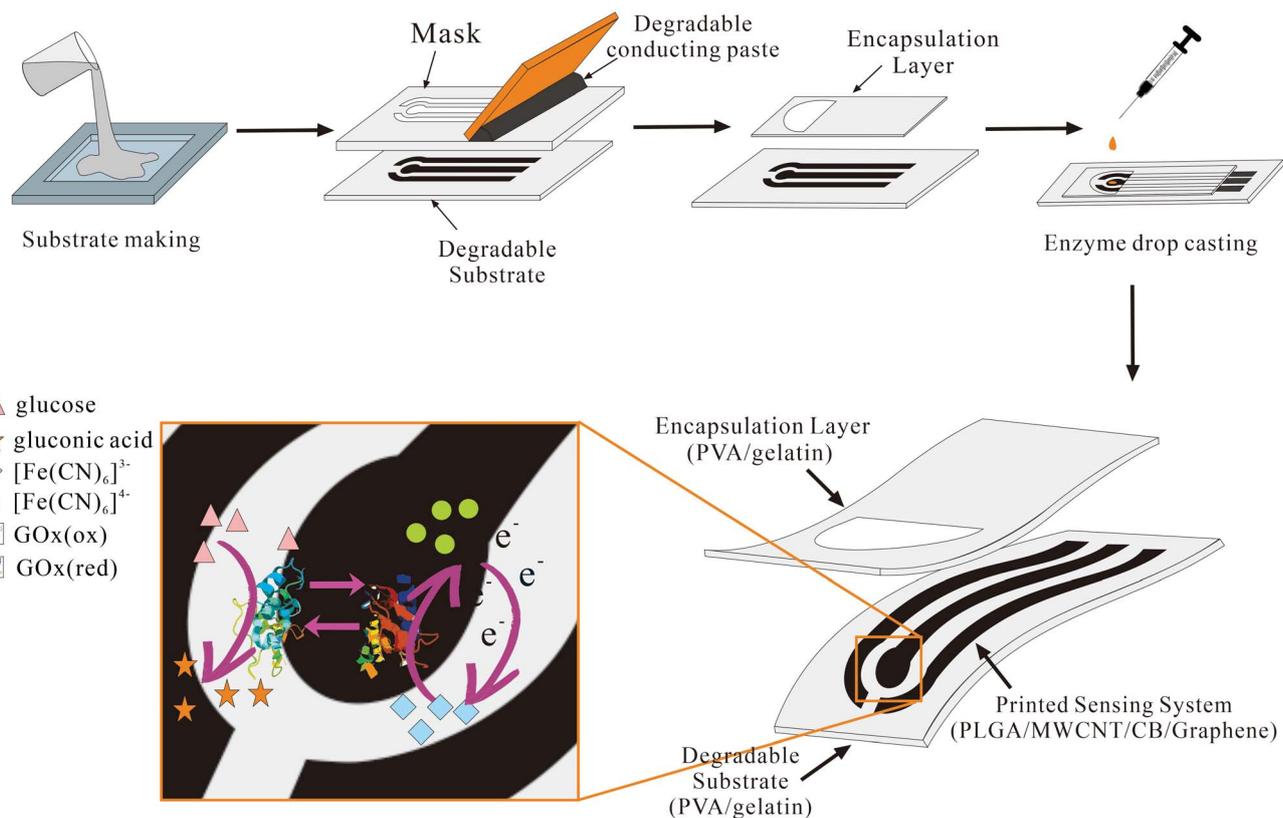

Fig. 1 Fabrication process of the fully transient electrochemical strip (up) and the working principle of glucose detection using $K_3Fe(CN)_6$ as an artificial mediator (down).

whole strip. The semicircle-shaped opening of the encapsulation layer plays an important role in controlling the reaction area and minimizing sample volume as well. Then with active sensing materials drop-casted onto the working electrode (WE), a transient electrochemical strip was completed (Fig. 2A). These strips with subsequent industrial packaging can be used in POCT for multi-detection. Fig. 2B was the simulated dissolution process after strips were discarded. After a four-day immersion in DI water, the strip dissolved in all levels indicating its in-time degradability. The detection-steady property is also validated by both morphology (Fig. S1†) and electrochemical manifestation (Fig. S2†). In the first five minutes of immersion, the sensing area stayed nearly unchanged, indicating its stability before minute five (at a time that most of the POCT detection will be finished). The conclusion could be verified again through the control experiment between PET-based strips and our transient strips. As we can observe from Fig. S2,† the curve of the commercial PET-based strips satisfies the equation of diffusion-controlled electrochemical detection process with a sharp current drop at the beginning and almost a horizontal line near the end, and the transient strip depicted a similar trend. However, the difference emerges at around 300 second with a distinct current drop of the transient strips compared to the expected curve (dotted line in blue). After 300 second, the current of transient strips keep on dropping, which to some extent violates the diffusion-controlled electrochemical module, indicating its instability after 5 minutes and its detection stability before this time point *vice versa*.

Dissolution process of degradable substrate

Widely used in the field of transient electronics, degradable materials can be divided into several classes including degradable conducting metals, degradable polymers, and biodegradable green materials. Here, we focus more on degradable polymers as ingredients for degradable substrates. Most typical degradable polymers are water-soluble polymers which are substituted or incorporated with hydrophilic groups into their backbone that can be dissolved, disperse or swell in water. For instance, sodium carboxymethyl cellulose (Na-CMC), poly(vinyl alcohol) (PVA), poly(lactic-*co*-glycolic acid) (PLGA) and poly(caprolactone) (PCL) have been previously studied as substrates. Na-CMC substrate is cheaply available and can be quick degradable.[15,25,31] PVA is an ideal substrate candidate for its multi-advantages including being non-toxic, non-carcinogenic, and soluble in many solvents. Generally, the solubility of PVA in the solution relies on the degree of polymerization and solution temperature. Researches show that the addition of gelatin to PVA polymer matrix is viable to regulate the compound's strength, a strength that is vital in strip making and should be strong enough to maintain strip shape, and solubility due to the presence of triple helixes in gelatin structure.[32] PLGA is a copolymer of PLA and PGA with a wide range of degradation rate, determined by the molecular weight together with the composition ratio of PLA and PGA. Specifically, the hydrophobicity of PLGA can be increased by the enhancement of PLA components, leading to a slower degradation process.[33] PCL is an alternative for substrate in the field of transient electronics as well.[13,34] In our case, a substrate with detection-

Fig. 2 (A) Images of the fully transient electrochemical strips. (B) Sequential dissolution images of a fully transient electrochemical strip in DI water (RT).
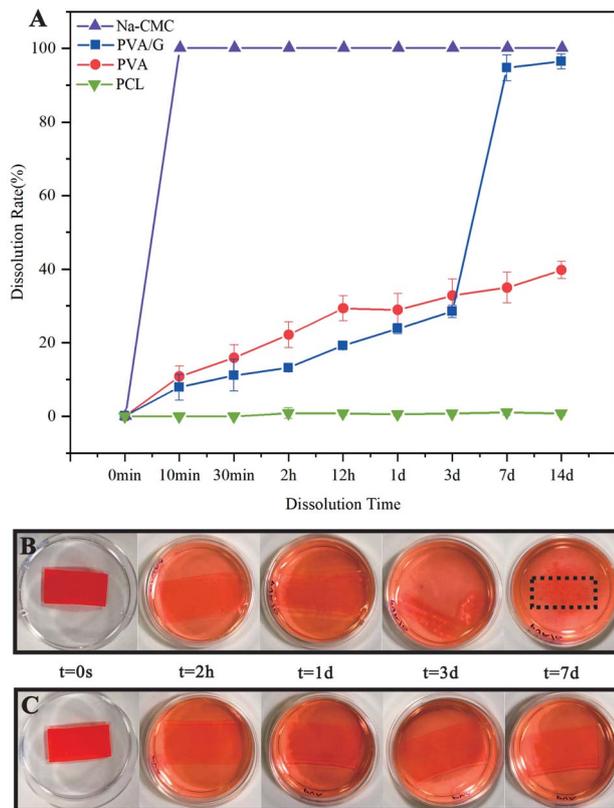
Fig. 3   Dissolution processes of degradable substrates. (A) Dissolution rate with time in DI water (RT) of four polymer–based substrates including Na–CMC, PVA, PVA/gelatin and PCL. (B) Optical images of PVA/gelatin substrate immersed in DI water (RT). (C) Optical images of PVA substrate immersed in DI water (RT).

steady and in-time degradable properties is required. Meanwhile, as a disposal strip, cost efficiency and broad manufacturing convenience should also be considered.

Here, the dissolution processes of four kinds of polymer-based substrates which are made from Na-CMC, PVA, PVA/gelatin and PCL were investigated (Fig. 3A). All the substrates were prepared by solution casting method in a Teflon mould, and the experiment was repeated for five times. As is shown from the curves in Fig. 3A, Na-CMC substrate was the first one to achieve full degradation in water (almost within 30 seconds) (Fig. S3†) while PCL stayed nearly unchanged during the whole process. PVA and PVA/gelatin substrates kept almost the same dissolution pace in the first three days with a lower rate of PVA/gelatin, confirming that the addition of gelatin does lower the swelling and dissolution process.[32] The difference emerged after seven days. The PVA/gelatin was nearly fully-dissolved leaving a cloudy solution behind while the PVA was still on its way to 50% degradation. One reasonable explanation for this phenomenon may lies in high gelatin and PVA ratio. Filled with much gelatin between the PVA polymer gaps (Fig. S4†), the PVA/gelatin substrate is more likely to be early dissolved since the solubility of gelatin in water (RT) distinct from that of PVA. Hence, the swelling gelatin disintegrated the PVA/gelatin

substrate making the whole structure to collapse. In order to eliminate the effect of residual water in substrate samples, all the substrates were pre-dried at 25 °C for 48 hours and the results noted in Fig. S5† indicate that the effect could be negligible. By comparing the optical images of substrate dissolution process in Fig. 3B (PVA/gelatin) and Fig. 3C (PVA), both of the substrates can preserve original shape for 2 hours which meets the requirement for electrochemical detection in the long-term watery environment. However, shape-preserving as PVA is, it cannot be dissolved timely, while PVA/gelatin reached its full-degradation in the day 7, claiming its qualification as a suitable substrate for transient electrochemical strips.

Morphology characterization of degradable paste

In the field of transient electronics, degradable metals mainly serve as degradable conducting traces combining with degradable substrate and encapsulation layer to make up an overall electronic system. Such degradable metal materials can be micro-fabricated onto a wide range of substrates through electron beam evaporation, magnetron sputtering, CVD or through printable metal inks/pastes.[6,9,25] However, the dissolution of these materials all involves hydrolysis reaction to form their corresponding hydroxides which contradict to the inert principle of the electrode during electrochemical detection process. Precisely speaking, the material for electrochemical electrodes should be chemically stable and well conductive during detection under watery condition. Such degradable metals can be too chemically active that the electrodes made from them may be dissolved before the detection process is completed. In traditional electrochemical systems, carbon-based materials are dominant in electrode making for their chemical inertness and excellent electrical conductivity. Multi-walled carbon nanotubes (MWCNTs), as a common one-dimensional carbon material, have assisted numerous sensors in achieving competitive sensitivity and linear range with its wire-like structure.[35,36] Nano-sized carbon black is frequently added into commercial carbon paste as an accessory ingredient to enhance conductivity.[37] Let alone graphene, the most emerging and promising carbon material in 21 century, which has brought the whole human science up to a new level.

Therefore, carbon materials above were blended to create a multi-dimensional structured carbon paste using PLGA as binder (Fig. 4A). We assume that in this structure, nanoscale carbon black (zero-dimensional) served as conductive filler in the gaps between MWCNTs (one-dimensional), and graphene (two-dimensional) worked as conductive plates holding up these decorated MWCNTs to strive for further conductivity improvement. The scanning electron microscopic images confirmed the conjecture. Fig. 4B exhibits the SEM structure of MWCNTs. Distinct gaps can be observed between the MWCNTs, which may lead to poor conductivity. With carbon black and graphene added, Fig. 4C and D display a clear multi-dimensional structure with carbon black particles filling the gaps held by graphene. To avoid the effect of PLGA's viscosity on imaging quality, the samples used for SEM were PLGA excluded.
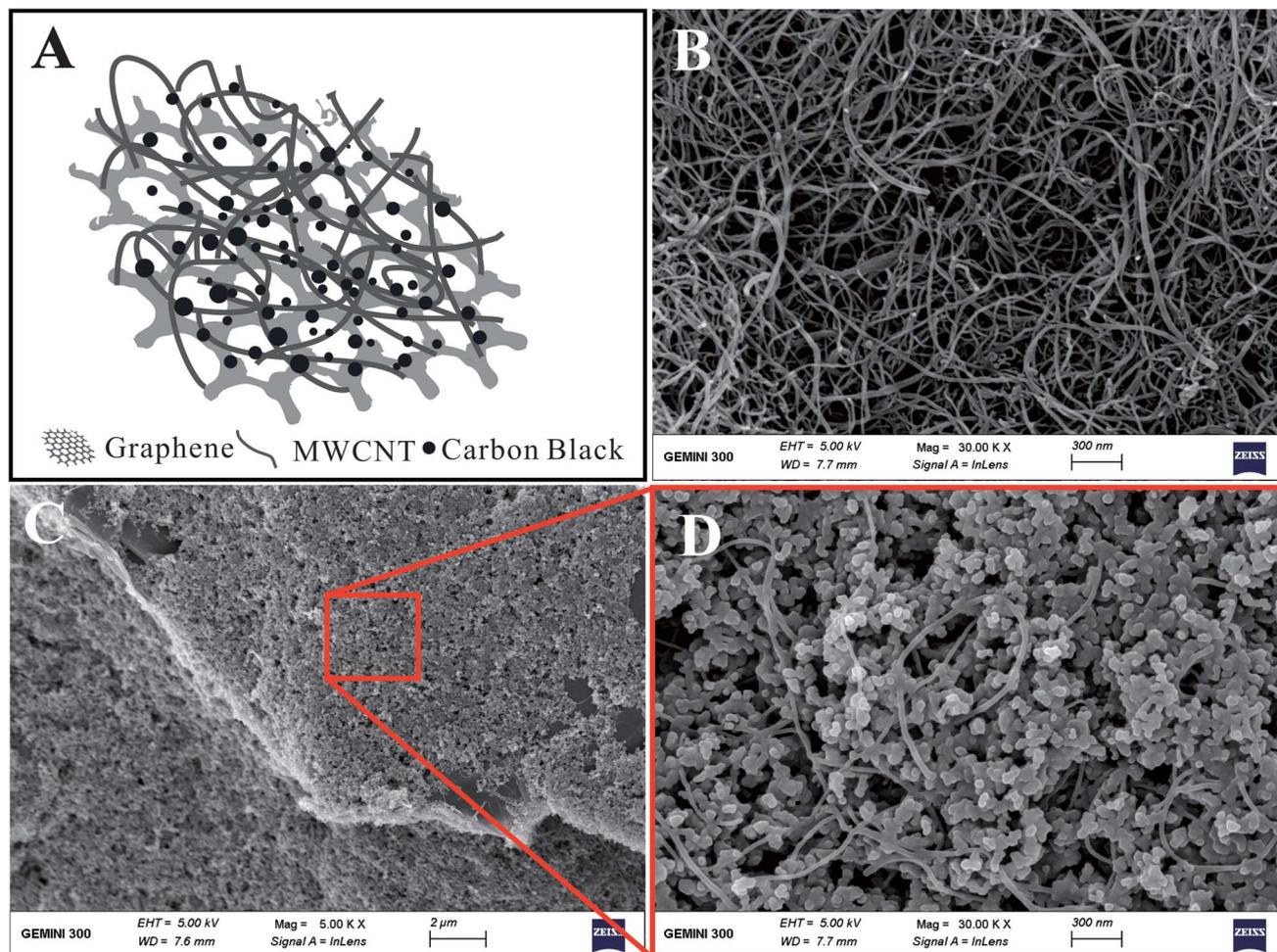
Fig. 4 (A) Schematic illustration of paste microstructure with carbon black as filler in MWCNTs gaps and graphene as conductive plate holding decorated MWCNTs. (B) SEM images of MWCNTs exhibiting distinct gaps. (C) SEM images of paste with MWCNTs/CB/graphene. (D) SEM images of CB-decorated MWCNTs on the graphene indicating a well-connected multi-dimensional structure.

Conductivity optimization of degradable paste

Viscous and degradable as PLGA is, this polymer cannot be conductive. Higher content of PLGA can lead to strong connections between conductive carbon-based materials but also a weaker conductivity. Explorations on different ratios of PLGA to carbon-based-materials were made trying to figure out the impact of PLGA on paste conductivity. The datum in Fig. 5A manifest that the conductivity decreases as the content of PLGA goes up. Yet it does not mean that the lesser PLGA is, the better the paste is. Cracks will appear in printed samples if too little PLGA is added (Fig. S6†), for it plays a connecting role between all composites (Fig. S7†). In consideration of conductivity and stability, the ratio PLGA : C = 2 was chosen as the optimized condition for later research. The relationship between paste conductivity and the ratio of carbon black to MWCNTs was also a part of the study (Fig. 5B). Although the conductivity changed slightly with adjusting the ratio of carbon black to MWCNTs, the lowest resistance was acquired when the ratio comes to four. Graphene was later added into the optimized paste, and it turned out to be more conductive, which proved the conjecture mentioned above again (Fig. S8†). All the experiments above

were repeated three times. Fig. 5C displays the dissolution process of degradable carbon paste in an alkaline solution using PET as substrates, which takes a much longer time than
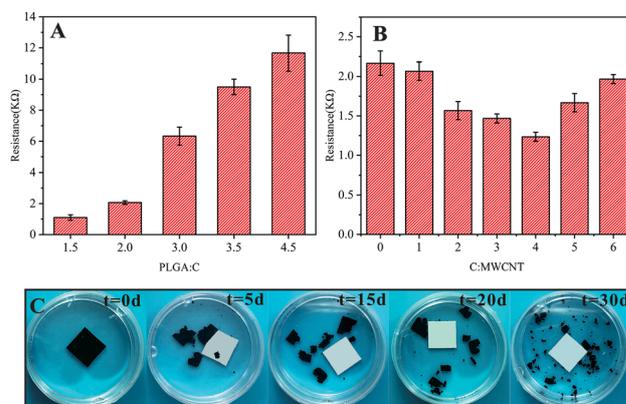

Fig. 5 (A) Resistance change with different ratios of PLGA to carbon materials. (B) Resistance change with different ratios of carbon black to MWCNTs. (C) Dissolution process of MWCNTs/CB/graphene paste on PET substrate in alkaline solution.
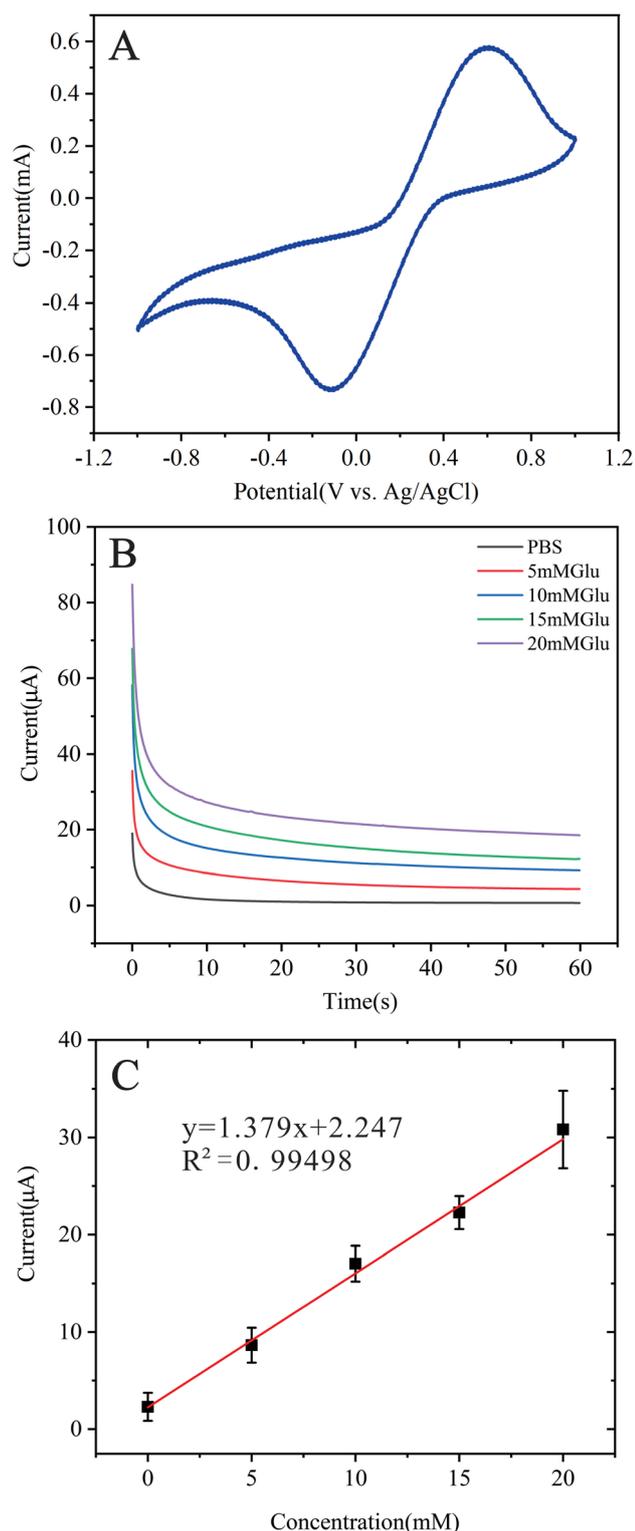
Fig. 6 Electrochemical performances of fully transient strips for glucose detection. (A) Cyclic voltammogram (CV) of strips in 50 mM $K_3Fe(CN)_6$ solution. Scan rate: 50 mV s^{-1}. (B) Typical amperometric responses of strips to glucose with different concentrations. (C) Calibration curve of the fully transient glucose sensors (error bar refers to sensor-to-sensor variation). The applied potential is 0.45 V vs. Ag/AgCl in all amperometric measurements.

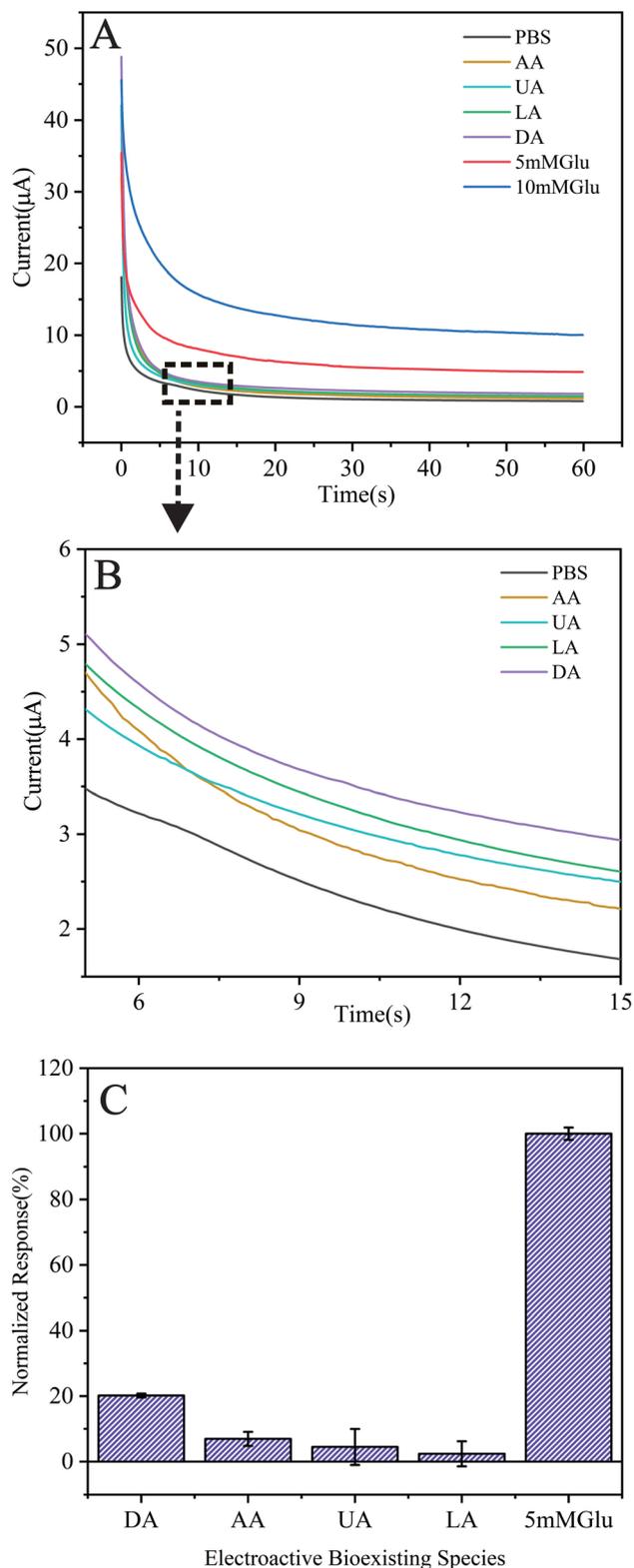Fig. 7 (A) Interference tests of fully transient strips in 100 μM AA, 100 μM DA, 100 μM LA and 50 μM UA respectively. (B) The detailed current response of four interference compared to PBS. (C) The normalized current signals comparing the interfering species to glucose. The applied potential is 0.45 V vs. Ag/AgCl in all amperometric measurements.

PVA/gelatin-based paste dissolution process in Fig. 2A. This is because different substrate materials can bring significant differences in paste dissolution process. With the substrates' disintegration or non-degradation, the dissolution rate can be accelerated or decelerated. In this case, the swelling and dissolution process of PVA/gelatin accelerated the paste dissolution rate since the paste stuck tightly onto the PVA/gelatin substrate.

Glucose detection using fully transient electrochemical sensors

As the main parameter in POCT detection, glucose detection using fully transient electrochemical electrodes was investigated (Fig. S9†). Cyclic voltammogram (CV) of transient electrodes was performed in 50 mM $K_3Fe(CN)_6$ solution (Fig. 6A). In the presence of $K_3Fe(CN)_6$, the transient electrodes showed prominent oxidation current ranging from 0.2 V *vs.* Ag/AgCl and reached a peak between 0.4 to 0.6 V *vs.* Ag/AgCl. While performing amperometric response of the transient electrodes, potential at 0.45 V *vs.* Ag/AgCl was used for sensing glucose in consideration of both reducing interference response current and increasing target response current. Fig. 6B exhibits the amperometric responses of the transient sensors under different concentrations of glucose solution. On the whole, the current increases linearly with glucose concentrations. Specifically, the relation between the current and the concentration can be described by eqn (4):

$$I = 1.379c + 2.247, (R^2 = 0.99498, N = 4) \quad (4)$$

where I (unit: μA) is the current chosen from amperometric response curve at ten second and c (unit: mM) is the glucose concentration. The amperometric currents demonstrated good linear relationship with the concentration of glucose from 0–20 mM. Based on the slope of this linear fit (Fig. 6C), the sensitivity of our fully transient electrochemical glucose electrodes is calculated as 14.33 μA mM^{-1} cm^{-2}. Another evaluation method testing the products after enzymatic reaction (eqn (2)) was also used to reassure the functionality of the transient electrodes in glucose detection (Fig. S10†).[38] Both results have suggested the application possibility towards glucose detection in human blood with such a wide linear range. For a better comprehension of fully transient electrochemical sensors, same measurements (Fig. S9 and S11†) using all-carbon-electrode fully transient sensors with degradable carbon CE and RE were also conducted, demonstrating the similar functionality towards glucose detection.

Anti-interfere capability of transient sensors

Nevertheless, in real human blood exists a considerable amount of oxidizable substances that can interfere with glucose detection. These interferents include ascorbic acid (AA), dopamine (DA), uric acid (UA), lactic acid (LA) and various other compounds. It is well known that the anti-interfere capability is such a valuable property that it may determine the sensor performance in real sample detection. Thus, the anti-interference property of transient glucose sensors was explored. Typically, the glucose level in human blood ranges from 3.0 mM to 8.0 mM, which is at least thirty times higher than the interfering substances (below 0.1 mM).[39] Here, we prepared four kinds of interfering species including 100 μM AA, 100 μM DA, 100 μM LA, and 50 μM UA and recorded their current responses respectively (Fig. 7A). The enlarged image from the rectangular is presented in Fig. 7B, where all the amperometric response curves of interferents are around base line (PBS) and lie distantly from the curve of 5 mM glucose, demonstrating low interference level of these substances during glucose detection. In Fig. 7C, the normalized current responses of AA (6.93%), UA (4.47%), and LA (2.39%) showed negligible influences towards glucose detection. However, we observed that the response ratio of DA (20.18%) is a bit higher than other interfering substances. According to some studies, DA possessed an extremely higher response than AA and UA at the same concentration, which to some extent explains the phenomenon here.[40] Still and all, the anti-interference capability towards DA of such transient electrochemical sensors is not ideal enough in practical application and further investigation will be made to strive for better performances. Another evaluation method using all-carbon-electrode fully transient sensors (Fig. S11†) demonstrated satisfying anti-interference capability, proving again the feasibility of the fully transient electrochemical sensors in practical application.

Recovery tests in serum samples

Besides, tests in bovine serum samples were performed to evaluate the practical application of transient glucose sensors. Samples with different glucose concentrations were prepared, and their actual glucose concentration changes were determined by a lab accurate glucose analyser. The fitted glucose concentration is calculated from the calibration curve. The measurement results are listed in Table 1. In all the samples, the recovery ratio between the fitted value and actual value ranges from 92.46% to 102.47% with RSD% value ($n = 3$) in the

Table 1 Determination of glucose concentration in blood serum samples using fully degradable electrochemical strips

Sample number	Added glucose concentration [mM]	Fitted concentration [mM]	Recovery [%]	RSD [%, $n = 3$]
1	3	2.77	92.46	5.35
2	5	5.12	102.47	3.87
3	8	7.89	98.72	4.02

range of 3.87–5.35% demonstrating its great potential in real human blood detection.

Conclusions

The transient electrochemical strips reported here suggest an approach to build a temporary system for eco-friendly POCT detection. A hybrid material of PVA and gelatin were chosen for substrates for its well detection-steady property and in-time degradability. Composed of MWCNTs/carbon black/graphene and PLGA, the mixed degradable carbon paste provides a possibility of obtaining well-conductive transient electrochemical strips. Satisfying linear detection range of glucose covering the normal blood glucose levels and favorable anti-interference capability were acquired using the transient electrochemical sensors. The good results in real sample detection experiment proved the probability of practical use of the transient electrochemical strips in clinical medicine not only for detection of glucose but also multi-parameters including uric acid, cholesterol and so on. Considering the dissolvable characteristic, further applications on implantable devices of these transient electrochemical sensors can be expected.

Conflicts of interest

There are no conflicts to declare.

Acknowledgements

References

1 J. E. Epping-Jordan, S. D. Pruitt, R. Bengoa and E. H. Wagner, *Qual. Saf. Health Care*, 2004, **13**, 299–305.

2 J. Piette, H. Valverde, N. Marinec, R. Jantz, K. Kamis, C. Lazo de la Vega, T. Wooley and B. Pinto, *Front. Public Health*, 2014, **2**, 1–10.

3 J. D. Newman and A. P. F. Turner, *Biosens. Bioelectron.*, 2005, **20**, 2435–2453.

4 I. D. Federation, *The global impact of diabetes*, https://www.idf.org/, accessed 14 July, 2019.

5 S.-W. Hwang, H. Tao, D.-H. Kim, H. Cheng, J.-K. Song, E. Rill, M. A. Brenckle, B. Panilaitis, S. M. Won, Y.-S. Kim, Y. M. Song, K. J. Yu, A. Ameen, R. Li, Y. Su, M. Yang, D. L. Kaplan, M. R. Zakin, M. J. Slepian, Y. Huang, F. G. Omenetto and J. A. Rogers, *Science*, 2012, **337**, 1640–1644.

6 L. Yin, H. Cheng, S. Mao, R. Haasch, Y. Liu, X. Xie, S.-W. Hwang, H. Jain, S.-K. Kang, Y. Su, R. Li, Y. Huang and J. A. Rogers, *Adv. Funct. Mater.*, 2014, **24**, 645–658.

7 S.-W. Hwang, S.-K. Kang, X. Huang, M. A. Brenckle, F. G. Omenetto and J. A. Rogers, *Adv. Mater.*, 2015, **27**, 47–52.

8 S.-K. Kang, G. Park, K. Kim, S.-W. Hwang, H. Cheng, J. Shin, S. Chung, M. Kim, L. Yin, J. C. Lee, K.-M. Lee and J. A. Rogers, *ACS Appl. Mater. Interfaces*, 2015, **7**, 9297–9305.

9 S.-K. Kang, S.-W. Hwang, H. Cheng, S. Yu, B. H. Kim, J.-H. Kim, Y. Huang and J. A. Rogers, *Adv. Funct. Mater.*, 2014, **24**, 4427–4434.

10 M. A. Brenckle, H. Cheng, S. Hwang, H. Tao, M. Paquette, D. L. Kaplan, J. A. Rogers, Y. Huang and F. G. Omenetto, *ACS Appl. Mater. Interfaces*, 2015, **7**, 19870–19875.

11 S.-K. Kang, R. K. J. Murphy, S.-W. Hwang, S. M. Lee, D. V. Harburg, N. A. Krueger, J. Shin, P. Gamble, H. Cheng, S. Yu, Z. Liu, J. G. McCall, M. Stephen, H. Ying, J. Kim, G. Park, R. C. Webb, C. H. Lee, S. Chung, D. S. Wie, A. D. Gujar, B. Vemulapalli, A. H. Kim, K.-M. Lee, J. Cheng, Y. Huang, S. H. Lee, P. V. Braun, W. Z. Ray and J. A. Rogers, *Nature*, 2016, **530**, 71.

12 K. Fu, Z. Wang, C. Yan, Z. Liu, Y. Yao, J. Dai, E. Hitz, Y. Wang, W. Luo, Y. Chen, M. Kim and L. Hu, *Adv. Energy Mater.*, 2016, **6**, 1502496.

13 H.-S. Kim, S. M. Yang, T.-M. Jang, N. Oh, H.-S. Kim and S.-W. Hwang, *Adv. Healthcare Mater.*, 2018, **7**, 1801071.

14 Z. Zhou, H. Mao, X. Wang, T. Sun, Q. Chang, Y. Chen, F. Xiu, Z. Liu, J. Liu and W. Huang, *Nanoscale*, 2018, **10**, 14824–14829.

15 B. K. Mahajan, X. Yu, W. Shou, H. Pan and X. Huang, *Small*, 2017, **13**, 1700065.

16 X. He, J. Zhang, W. Wang, W. Xuan, X. Wang, Q. Zhang, C. G. Smith and J. Luo, *ACS Appl. Mater. Interfaces*, 2016, **8**, 10954–10960.

17 S. M. Won, J. Koo, K. E. Crawford, A. D. Mickle, Y. Xue, S. Min, L. A. McIlvried, Y. Yan, S. B. Kim, S. M. Lee, B. H. Kim, H. Jang, M. R. MacEwan, Y. Huang, R. W. Gereau IV and J. A. Rogers, *Adv. Funct. Mater.*, 2018, **28**, 1801819.

18 J. Xu, X. Zhao, Z. Wang, H. Xu, J. Hu, J. Ma and Y. Liu, *Small*, 2019, **15**, 1803970.

19 S.-W. Hwang, D.-H. Kim, H. Tao, T.-i. Kim, S. Kim, K. J. Yu, B. Panilaitis, J.-W. Jeong, J.-K. Song, F. G. Omenetto and J. A. Rogers, *Adv. Funct. Mater.*, 2013, **23**, 4087–4093.

20 C. M. Boutry, A. Nguyen, Q. O. Lawal, A. Chortos, S. Rondeau-Gagné and Z. Bao, *Adv. Mater.*, 2015, **27**, 6954–6961.

21 G. A. Salvatore, J. Sülzle, F. Dalla Valle, G. Cantarella, F. Robotti, P. Jokic, S. Knobelspies, A. Daus, L. Büthe, L. Petti, N. Kirchgessner, R. Hopf, M. Magno and G. Tröster, *Adv. Funct. Mater.*, 2017, **27**, 1702390.

22 S.-W. Hwang, C. H. Lee, H. Cheng, J.-W. Jeong, S.-K. Kang, J.-H. Kim, J. Shin, J. Yang, Z. Liu, G. A. Ameer, Y. Huang and J. A. Rogers, *Nano Lett.*, 2015, **15**, 2801–2808.

23 L. Yin, X. Huang, H. Xu, Y. Zhang, J. Lam, J. Cheng and J. A. Rogers, *Adv. Mater.*, 2014, **26**, 3879–3884.

24 G. Lee, S.-K. Kang, S. M. Won, P. Gutruf, Y. R. Jeong, J. Koo, S.-S. Lee, J. A. Rogers and J. S. Ha, *Adv. Energy Mater.*, 2017, **7**, 1700157.

25 X. Huang, Y. Liu, S.-W. Hwang, S.-K. Kang, D. Patnaik, J. F. Cortes and J. A. Rogers, *Adv. Mater.*, 2014, **26**, 7371–7377.

26 W. Jiang, H. Li, Z. Liu, Z. Li, J. Tian, B. Shi, Y. Zou, H. Ouyang, C. Zhao, L. Zhao, R. Sun, H. Zheng, Y. Fan, Z. L. Wang and Z. Li, *Adv. Mater.*, 2018, **30**, 1801895.

27 S.-W. Hwang, J.-K. Song, X. Huang, H. Cheng, S.-K. Kang, B. H. Kim, J.-H. Kim, S. Yu, Y. Huang and J. A. Rogers, *Adv. Mater.*, 2014, **26**, 3905–3911.

28 L. General Life Biotechnology Co., http://www.glbiotech.com.tw/product_view.php?item=5, accessed 11 Nov, 2019.

29 H. T. Ratte, *Environ. Toxicol. Chem.*, 1999, **18**, 89–108.

30 J. Wang, *Chem. Rev.*, 2008, **108**, 814–825.

31 W. Shou, B. K. Mahajan, B. Ludwig, X. Yu, J. Staggs, X. Huang and H. Pan, *Adv. Mater.*, 2017, **29**, 1700172.

32 H. Acar, S. Çınar, M. Thunga, M. R. Kessler, N. Hashemi and R. Montazami, *Adv. Funct. Mater.*, 2014, **24**, 4135–4143.

33 P. Gentile, V. Chiono, I. Carmagnola and P. V. Hatton, *Int. J. Mol. Sci.*, 2014, **15**, 3640–3659.

34 Y. Gao, K. Sim, X. Yan, J. Jiang, J. Xie and C. Yu, *Sci. Rep.*, 2017, **7**, 947.

35 D. Maity and R. T. R. Kumar, *Biosens. Bioelectron.*, 2019, **130**, 307–314.

36 L. Yao, J. Teng, M. Zhu, L. Zheng, Y. Zhong, G. Liu, F. Xue and W. Chen, *Biosens. Bioelectron.*, 2016, **85**, 331–336.

37 J. H. Zhou and H. J. Yin, *China Pat.*, CN201510034134.X, 2015.

38 Z. Nie, F. Deiss, X. Liu, O. Akbulut and G. M. Whitesides, *Lab Chip*, 2010, **10**, 3163–3169.

39 S. Lin, W. Feng, X. Miao, X. Zhang, S. Chen, Y. Chen, W. Wang and Y. Zhang, *Biosens. Bioelectron.*, 2018, **110**, 89–96.

40 H. Yang, J. Zhao, M. Qiu, P. Sun, D. Han, L. Niu and G. Cui, *Biosens. Bioelectron.*, 2019, **124–125**, 191–198.